Single-Cell Separation

Shilpi Pandey, Ninad Mehendale, and Debjani Paul

Contents

Abstract

Advances in both basic cell biology and point-of-care diagnostic technology led to the need for reliable, accurate, and fast techniques to separate single cells from a heterogeneous mixture. Conventional cell separation techniques, such as fluorescence-activated cell sorting (FACS) and magnetic-activated cell sorting (MACS), are very efficient methods. However, these techniques are generally expensive, require bulky equipment, and are not suitable for use in field settings. On the other hand, microfluidic technology matches the performance of existing techniques, while being more portable and suitable for field use. In this chapter,

S. Pandey · N. Mehendale · D. Paul (✉)
Department of Biosciences and Bioengineering, Indian Institute of Technology Bombay, Mumbai, Maharashtra, India
e-mail: shilpi.pandey@iitb.ac.in; ninad.mehedale@iitb.ac.in; debjani.paul@iitb.ac.in

we discuss the working principles and illustrate some applications of various established and emerging microfluidic techniques. The emphasis of this chapter is more on the recent advancement in the field of microfluidics for rare or single-cell separation.

Introduction

Isolating rare cells from complex samples is an essential requirement for many biological and clinical applications. For instance, fetal cells present in maternal blood can be used for noninvasive prenatal testing. The frequency of fetal cells compared to the maternal mononuclear cells can vary a lot but is estimated to be approximately 10^{-5} to 10^{-7} (Wachtel et al. 2001). Isolating these cells from the mother's blood is the first step for fetal genetic testing. Cancer is another example of a disease where a capturing rare cell is an important requirement for diagnosis. Most deaths in cancer occur due to metastasis, a mechanism by which cells from the primary tumor travel to the other organs through the circulatory system. There are typically one to ten circulating tumor cells (CTC) in 1 ml of whole blood, and these need to be detected to understand the spread of the disease. Personalized medicine is another rapidly growing area, where isolation of hematopoietic stem cells from patients is required to provide autologous treatments.

Single-cell separation and analysis techniques are important due to the inherent heterogeneity of cell populations. Single-cell analysis can range from the measurement of the nucleic acid levels to the study of the proteomic and metabolomic characteristics of the cells. Conventional techniques can only measure the average properties of a cell population, which leads to a loss of valuable information from the rare cells present in that population. Moreover, owing to the time dependence of different transcriptional and signaling processes, ensemble averages fail to capture the cellular dynamics.

In both basic and clinical research, single-cell separation is mainly performed using conventional techniques, such as fluorescence-activated cell sorting (FACS), magnetic-activated cell sorting (MACS), laser capture microdissection (LCM), manual cell picking, etc. (Miltenyi et al. 1990; Datta et al. 2015; Hu et al. 2016). Currently, FACS is the benchmark technology for cell sorting. It is robust and automated and has a good throughput (~10,000–50,000 cells/s) for most research applications. However, the throughput of FACS is not high enough compared to a bulk sorting technique like centrifugation. Hence, the use of FACS for routine clinical applications, where millions of cells need to be processed in a relatively short period of time, is rather limited. Most conventional sorting techniques require highly skilled technicians, large volumes of samples, and well-equipped facilities. The equipment required for FACS has a large footprint and is expensive (>$100,000) (Lee et al. 2017). As a result, there has been a strong need for a next-generation technology for single-cell separation with high reliability, low cost, portability, higher speed of sorting for rare cells, and reduced risk of biohazards due to exposure to aerosols during sample preparation. Microfluidics is an emerging technology

which works with low sample volumes (~μL – pL) and can address most of the problems faced by the conventional techniques. Microfluidic cell separation technologies, such as hydrodynamic separation, deterministic lateral displacement, field flow fractionation, etc., have been extensively demonstrated for sorting, counting, and analyzing the contents of single cells of interest.

The performance of various cell separation techniques can be described by separation purity, throughput, sample recovery, and the enrichment factor. Purity is defined as the ratio of the number of target cells to the total number of sorted cells (counted at the outlet). Throughput is measured by the total output sample volume collected per unit time. The ratio of the total number of cells collected at the outlet to the total number of cells at the inlet is called recovery. It is a measure of the loss of cells inside the device. The enrichment factor is given by the Eq. 1.

$$\text{Enrichment factor} = \frac{\dfrac{\text{Number of target cells at the outlet}}{\text{Total number of cells at the outlet}}}{\dfrac{\text{Number of target cells at the inlet}}{\text{Total number of cells at the inlet}}} \tag{1}$$

Each cell separation technique has distinct advantages and disadvantages. Often, a user needs to balance different performance parameters, leading to trade-offs. This chapter begins with an overview of some of the conventional techniques for single-cell separation. The chapter then focuses on the microfluidic single-cell separation techniques. These techniques can broadly be divided into two classes: (a) passive techniques that do not require any external fields and (b) active techniques that sort cells with the help of an external field (e.g., electric, magnetic, optical, acoustic, etc.). Finally, the performances of the different passive and active microfluidic sorting techniques are compared.

Conventional Cell Separation Techniques

Conventional and microfluidic cell separation techniques (Fig. 1) can be classified into two categories: (a) techniques that exploit the difference in physical properties (e.g., size, density, deformability, electric charge, etc.) of cells in a heterogeneous population and (b) labeled techniques which rely on the presence of specific biological markers on the cells (e.g., antigens, recombinant proteins, etc.). The techniques which are based on the physical properties are also known as label-free techniques. The most common label-free technique for separating the components of blood is density gradient centrifugation. Although it is strictly not a single-cell separation technique, it can be used as an enrichment step to speed up the subsequent process of single-cell isolation. Common single-cell sorting techniques like FACS and MACS require the use of labels.
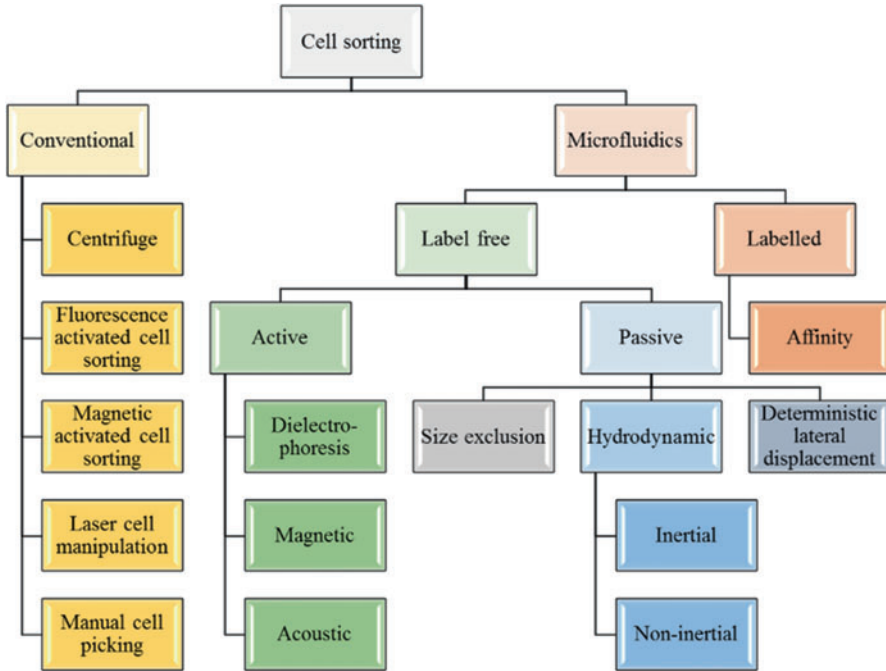
Fig. 1 Classification of different cell separation techniques

Centrifugation

Centrifugation is the most commonly used technique to separate the different components of blood. It is widely used in both research laboratories and clinical settings. In centrifugation (Fig. 2a), the difference in the densities of various blood components (plasma, red blood cells, etc.) is exploited. About 5–10 mL blood is loaded into a test tube and spun at a high speed. As shown in Fig. 2b, after centrifugation, dense RBCs settle down at the bottom of the test tube. Plasma settles at the topmost layer, while platelets and WBC are found in an intermediate layer (buffy coat).

A secondary centrifugation of the buffy coat is needed to separate the WBCs and the platelets. For this purpose, a special density gradient separation media (Hi-sep) is added to the buffy coat prior to spinning. Although centrifugation cannot separate individual rare cells, it is often used as an enrichment step before performing single-cell separation. For instance, Nagrath et al. used centrifugation as a preliminary sample preparation step prior to capturing CTCs from lysed blood using the CTC-chip (Nagrath et al. 2007).
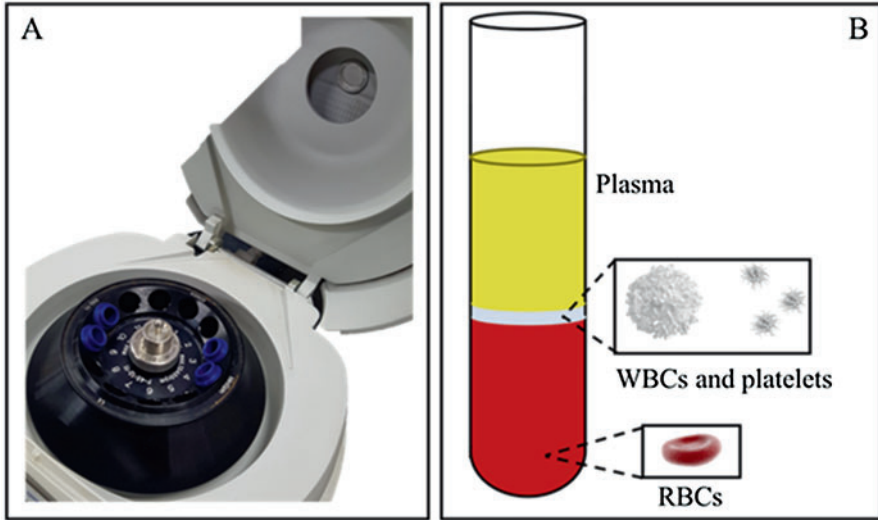
Fig. 2 Centrifugation used for separation of the components of blood. (**a**) Photo of a small tabletop centrifuge showing the slots for holding sample tubes. (**b**) Schematic diagram of a test tube showing the positions of different blood components after centrifugation. RBCs settle at the bottom, while plasma settles at the top. A buffy coat containing WBCs and platelets lies between the RBC and the plasma layers

Fluorescence-Activated Cell Sorting

FACS was first developed by Bonner, Hulett, Sweet, and Herzenberg (Bonner et al. 1972; Herzenberg and Sweet 1976; Hulett et al. 1969). It was the first cell sorting technique to be commercialized by Becton Dickinson Immunocytometry Systems in the 1970s. FACS is still the most widely used cell sorting technique. According to a review published in 2002, approximately 30,000 sorters and analyzers were estimated to be in use throughout the world (Herzenberg et al. 2002). The principle of operation of FACS is based on both fluorescence and the light scattering properties of individual cells. Light scattering is used to analyze cell parameters, such as size (forward scatter) and internal structure (side scatter). Since many cells do not have an inherent fluorescence, they are tagged with fluorophore-conjugated antibodies that bind to cell markers. Cells can also be made to express recombinant fluorescent proteins, such as green fluorescent protein (GFP).

In FACS (Fig. 3), the sample is encased by a sheath fluid and then focused into a narrow stream by a nozzle. The sample flow is adjusted such that the separation between the cells is large compared to the size of the cell, and only one cell is

Fig. 3 Fluorescence-activated cell sorting (FACS), in which cells are first focused such that only one cell is detected by the laser at a time. The detected cells are then enclosed in a drop, given an electric charge, and then separated by the deflector plates into different categories
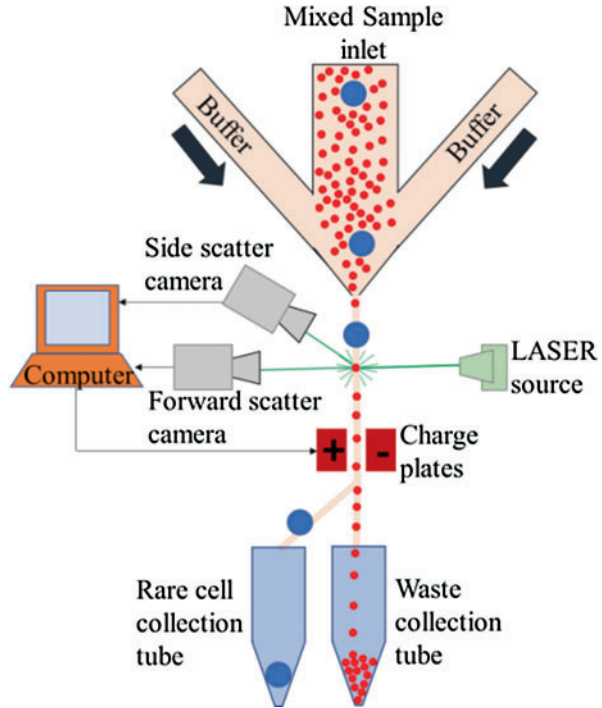
detected at a time. In the detection region, a laser excites the fluorescently tagged antibodies. The fluorescence and scatter signals from each cell are captured by multiple detectors. Once a cell passes the detection region, the stream is broken into droplets such that each droplet contains a single cell. Electric charge (negative or positive) is applied on the droplet based on the fluorescence signal of the cell it contains. Using electrostatic deflection, the charged droplet is led to a tube for further analysis.

FACS allows users to target multiple markers in the same experiment. The latest FACS systems allow up to 18 markers to be detected simultaneously with the help of 6 lasers and 20 detectors. But the technique requires extensive sample preparation. Predictably, the increase in the number of markers results in an increase in the system complexity and the equipment cost. FACS needs a relatively large number of cells (~ tens of thousands) to run an experiment effectively. In spite of these limitations, FACS is still the most widely used single-cell sorting technique.

Magnetic-Activated Cell Sorting

Magnetic-activated cell sorting (MACS) (Miltenyi et al. 1990) was developed to address the throughput limitations of FACS. In MACS (Fig. 4), antibody-coated magnetic beads (~100 nm diameter) specifically bind to a particular protein on the
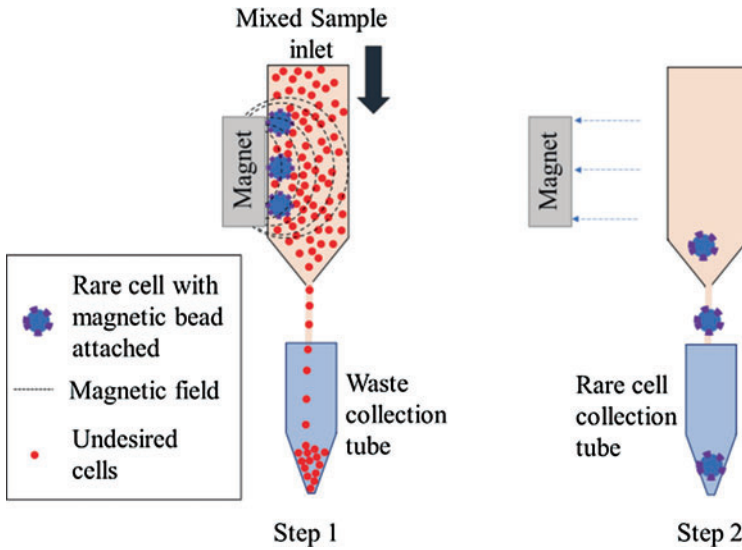
Fig. 4 Magnetically activated cell sorting (MACS) is achieved by attaching antibody-coated magnetic nanometer-sized beads to the cells of interest

surface of the desired cell. The magnetically tagged cells are passed through a steel wool column placed in a magnetic field gradient formed by permanent magnets. The labeled cells are captured by the column in the presence of the magnetic field, while unlabelled cells are washed away. Cells attached to the column can be eluted by turning off the magnetic field. During enrichment (also known as the positive separation), the desired cells are labeled with the coated magnetic beads, and the unlabelled cells are discarded. In case of depletion (also known as negative separation), the unwanted cells are labeled and captured by the magnetic field.

As discussed by (Miltenyi et al. 1990), the size of the magnetic particles must be carefully chosen. Large magnetic particles (size >0.5 µm) can respond well to a simple (non-gradient) magnetic field, but they lead to cell aggregation and decrease the cell viability. It becomes difficult to detach the bound cells, and consequently, the process can only be used for cell depletion. On the other hand, smaller particles (size <0.5 µm) attach much faster to the cells, do not aggregate, or change the properties of the cells. However, their response to the external magnetic field is slow leading to longer separation times. To address this problem, MACS uses small superparamagnetic particles in conjunction with a high-gradient magnetic field. As a result, both depletion and enrichment of cells can be performed using MACS.

MACS is usually faster compared to FACS as it does not interrogate cells one by one. However, unlike FACS, it can only target the cell surface markers. It cannot distinguish between high or low expression of the same surface marker. MACS-compatible magnetic antibodies are less readily available compared to fluorescently labeled antibodies. Finally, MACS can sort cells expressing a single marker at a time (either by positive or negative selection). In case certain rare cells need to be separated based on their expression of two or more markers, it would potentially
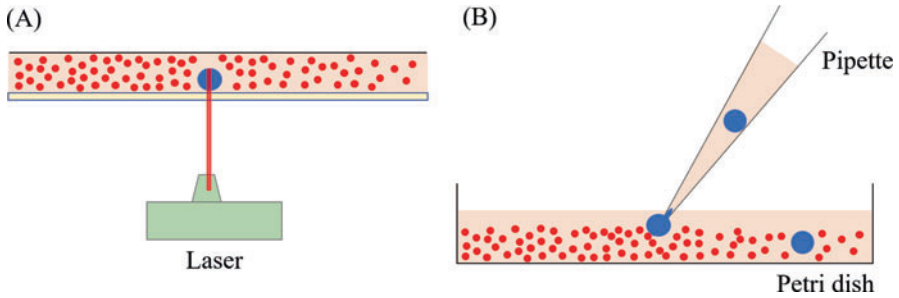
Fig. 5 (**a**) In laser capture microdissection, a cell is removed from a tissue sample by local ablation using a laser. (**b**) In manual cell picking, a micropipette attached to a micromanipulator is used to pick up the target cell

need multiple stages of MACS to be performed. MACS can often be used to enrich cells prior to FACS by using both fluorescent and magnetic-labeled antibodies (Miltenyi et al. 1990).

Laser Capture Microdissection

Laser capture microdissection (LCM), depicted in Fig. 5a, was first developed at the National Institutes of Health, Bethesda (Emmert-Buck et al. 1996). It can isolate the target cells from dehydrated tissue samples fixed on microscope slides. The main components of an LCM instrument are a vacuum chuck to immobilize the slide, an inverted microscope to see the cells, and a laser fitted with a control unit. The laser beam diameter ranges from 7 μm to 15 μm. The cell of interest in the tissue sample is first visualized on the slide using the inverted microscope. Then an LCM cap attached to a thin transparent thermoplastic film is lowered on the tissue. A focused laser beam is used to locally melt the thermoplastic film and fuse it to the cell just beneath it. The cap, with the cell of interest sticking to the film, is then moved away. The separated cells are collected into a micro centrifuge tube containing a suitable buffer solution and analyzed. LCM raises the temperature of the cell membrane to ~90 °C for only a few milliseconds, thereby leaving the biomolecules of interest inside the cell undamaged (Fend and Raffeld 2000). The most important requirement of LCM is the correct identification of the cell of interest in the tissue sample by microscopy. It requires trained and highly skilled users to perform the process. Another limitation is that due to the somewhat larger spot size compared to the size of a single cell, often other adjacent cells are also captured (Table 1).

Manual Cell Picking

Manual cell picking (Fig. 5b) requires an inverted microscope, ultrathin glass micropipettes for cell aspiration, and a motorized movable mechanical stage for positioning the micropipette. The cell suspension is first observed under the

Table 1 Comparison of conventional cell separation techniques

Method	Mechanism	Advantage	Disadvantage	Complexity
Centrifugation	Gravity	Easy	Not suitable for single-cell separation	Low
Fluorescence-activated cell sorting (FACS)	Fluorescence	Multiple surface markers	Extensive sample preparation required	High
Magnetic-activated cell sorting (MACS)	Magnetic field	High throughput	Separates only two types of cells at a time	High
Laser capture microdissection	Laser ablation	Works with tissue samples	Contamination from adjacent cells	Intermediate
Manual picking	Micropipette aspiration	Works with prokaryotic and eukaryotic cells	Skilled technician required	Low

microscope, and the micromanipulator is positioned near the cell of interest. The operator then lifts the cell by gentle aspiration using a micropipette. The isolated cells are transferred to a tube for further analysis. Unlike LCM, which works with fixed and dehydrated tissue samples, this technique can be used to isolate live cells from cultures. It can even be used to isolate bacteria. Though this technique is simple and quite common, it requires skilled professionals and has a very limited through-put (Hu et al. 2016).

Microfluidic Single-Cell Separation Techniques

Microfluidic devices (Beebe et al. 2002) operate at very low Reynolds numbers (Re) due to their micron-sized channel dimensions. As a result, the fluid flow in these channels is laminar. The laminar flow can be exploited to perform a number of operations, such as hydrodynamic flow focusing, protein patterning inside a microchannel, hydrodynamic separation of cells according to their sizes, etc. The most important application of microfluidics so far has been in developing lab-on-a-chip (LOC) devices. LOC devices offer numerous advantages over conventional benchtop techniques including low sample volumes, large surface-to-volume ratios leading to faster reactions and better heat dissipation, automation, and integrated sample handling capabilities. These systems can be fabricated using a wide range of materials, such as silicon, glass, thermoplastics, and elastomers (such as polydimethylsiloxane).

The lateral dimensions of microfluidic channels can be matched with the dimensions of cells (ranging from a few microns to tens of microns), making these devices particularly suitable for single-cell analysis (Stone and Kim 2001). A wide variety of microfluidic techniques for single-cell separation have been reported in the literature. These techniques can be divided into two classes: (a) passive separation

techniques that exploit the hydrodynamics of flow or the presence of obstacles inside the device and (b) active separation techniques that require the use of external fields. These two classes of separation techniques can be performed either with labels (e.g., antibodies, recombinant fluorescent proteins, aptamers, etc.) or without labels. Accordingly, these are called labeled or label-free separation techniques, respectively. In this section we describe some of the common label-free passive and active separation techniques. Finally, we describe some techniques using labels in the section on affinity-based separation. We do not cover droplet-based cell separation techniques in this section.

Microfluidic Passive Separation Techniques

Filter-Based Separation

Microfluidic filters separate cells based on their size and deformability. The feature sizes in microfabricated filters can be more precisely controlled to match the dimensions of single cells compared to macroscale filters. We discuss three types of microscale filters here: (a) weirs, (b) micropillars (cross-flow and dead-end filtration), and (c) membranes.

Figure 6a shows a schematic diagram of a *weir-type* cell separator (Ji et al. 2008). A weir is a single pillar, directly placed in the flow path, perpendicular to the flow. The height of the weir is smaller than the channel height. Cells smaller in size than the gap between the channel and the weir can pass through, while larger cells are stopped. A weir filter requires at least two-level lithography as the heights of the weir and the channel are different. The performance of a weir filter can be further improved using multilevel lithography, where the gap between the top surface of the channel and the weir height goes on reducing with each successive weir. This is called a trench-type filter. A major problem in this design is that of clogging of larger cells. If the large cells are deformable, they can sometimes squeeze through the gap between the weir and the channel, thereby reducing the filtration purity. Brody and others (Brody et al. 1996) proposed first time plasma separation from whole blood using microfabricated filter device. There is a report (Wilding et al. 1998) where WBCs from blood were captured using weirs and then the DNA from the trapped WBCs was used for PCR amplification in the same device. This kind of filter is usually used for separating plasma from whole blood. Due to the small size of the planar slit, plasma is obtained in very small volumes (~nL) (Brody et al. 1996; Crowley and Pizziconi 2005).

Pillar-type filtration employs a number of microfabricated posts inside a channel with varying gaps between the posts depending on the cell types to be sorted. Unlike weirs, the height of these pillars is the same as the channel height, making it possible to fabricate these devices in a single lithography step. There are two approaches under this technique: (a) dead-end filtration, (b) cross-flow filtration.

In *dead-end filter* (Ji et al. 2008) designs (Fig. 6b), the fluid flow is perpendicular to an array of microfabricated posts. The gap between the pillars is adjusted to
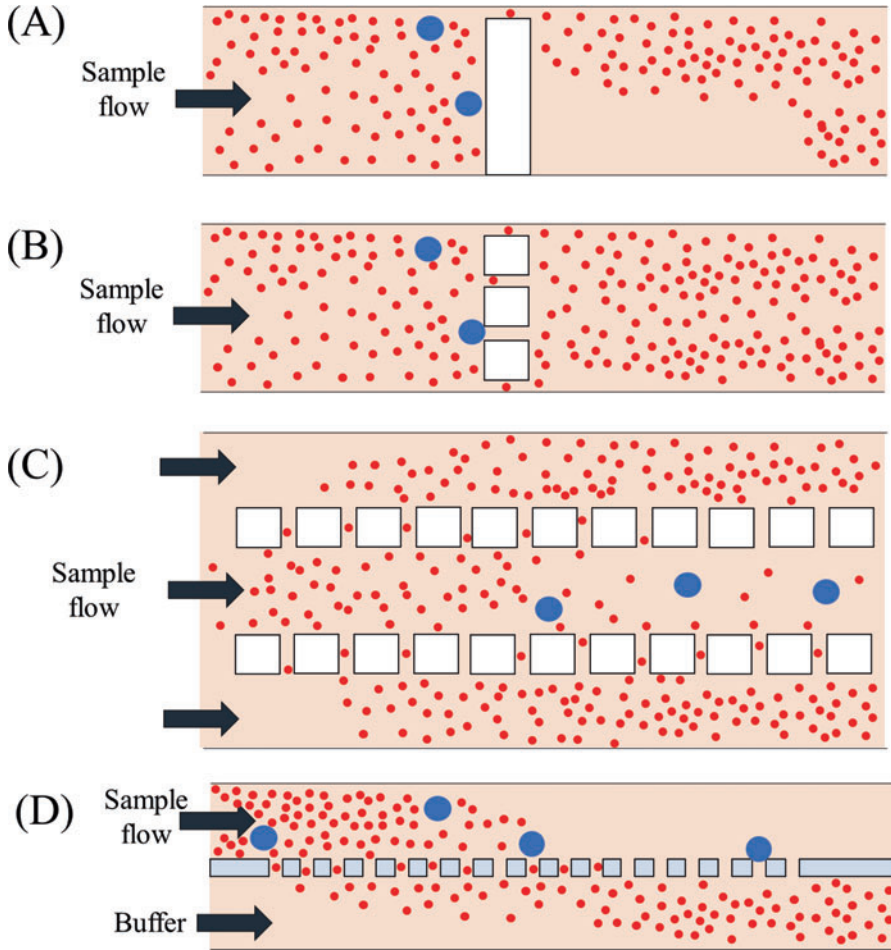
Fig. 6 Schematic diagram explaining different filter-based cell sorting methods. (**a**) Weir filter (side view). (**b**) Dead-end pillar filter (top view). (**c**) Cross-flow filter (top view). (**d**) Membrane filter (side view)

be smaller than the size of the cells to be trapped. However, the efficiency of dead-end pillar devices decreases over time as larger cells get trapped between the pillars. The stuck cells can be dislodged using a reverse flow, which again mixes the separated cells to an extent. To address the clogging problem and to improve the selectivity of cell separation, some groups have shaped the pillar gaps in the form of ratchets and reversed the flow periodically (McFaul et al. 2012).

To overcome the problem of cell clogging, *cross-flow filters* (Chen et al. 2008; VanDelinder and Groisman 2006) were designed. As shown in Fig. 6c, here the fluid flows in a direction parallel to the pillars. The larger particles remain in the main flow, while the smaller particles can enter the cross flow through the gaps between

the pillars. As particles prefer to take the path of the lowest hydrodynamic resistance, many small target particles also remain in the main flow instead of following the cross flow. Hence, cross-flow filters are not suitable for selective isolation of large rare cells. Low selectivity and a large device footprint are some problems of the cross-flow filter design. A report demonstrated the use of pulsatile flow (VanDelinder and Groisman 2007) to increase the efficiency of cross-flow microfiltration.

Like the cross-flow pillar design, a cross-flow weir filter (Chen et al. 2008) has also been reported. This device was fabricated in silicon using two-level lithography and deep reactive-ion etching (DRIE). The cross-flow weir filter demonstrated better RBC removal and WBC capture efficiencies for the same channel length and sample dilution compared to the cross-flow pillar filter. The RBC removal efficiency increased from 85.3% to 93.3% for 100X diluted blood, while the WBC capture efficiency was improved from 8% to 27.4%.

The *membrane filter* (Songjaroen et al. 2012), shown in Fig. 6d, is one of the simplest sorting mechanisms, consisting of a thin membrane with pores. Membrane filters suffer heavily from clogging by the trapped cells. The fabrication of the filter is also complex because it requires multiple lithography steps. Early membrane filters were fabricated with cylindrical pores, which led to the retention of nontarget cells. Tang and others (Tang et al. 2014) improved the design of microfilters by making the pores conical and integrated it with cross-flow injectors to allow nontarget cells to leave the device. The cells were introduced into the filter from the narrow part of the conical pore, allowing larger and stiffer cells to be trapped, while the smaller and more deformable cells passed through. They demonstrated its use by capturing circulating tumor cells (CTCs). They observed that the performance of the device strongly depends on the cell type and recommended that the pore size be closely matched to the nuclei diameter of the tumor cells for improved performance.

Ji and others (Ji et al. 2008) have compared the performances of silicon-based weir, membrane, dead-end pillar, and cross-flow pillar filters for the separation of WBCs from RBCs. The pore size of the membrane filters or the gap between the pillars was set at 3.5 μm in all four designs. They concluded that the cross-flow filtration technique performs the best with a capacity to handle whole blood volumes >300 μl and an efficiency of >70%–80% for trapping WBCs.

To balance the issues of increased separation efficiency with clogging-free operation, several variations on these primary design types have been reported. These approaches are passive (i.e., they do not require external energy sources), and the devices can be fabricated in a single lithography step. Mehendale et al. (2018) developed a radial pillar device (RAPID) design for simultaneous separation of multisized particles by combining the advantages of cross-flow and dead-end pillar filters. Here the pillars were arranged in concentric circles in three zones around a central inlet. The pillar gaps were decreased progressively in each zone according to the size of the particles to be captured. An angular displacement between the successive rows of pillars in the middle zone and the presence of a cross-flow outlet prevented clogging of this device by continuously removing

the undesired particles. They demonstrated simultaneous separation of 10 μm and 2 μm polystyrene beads from a mixture of 2 μm, 7 μm, and 10 μm beads with a high throughput (3 ml/min) in a single experiment. Another group (Mohamed et al. 2007) adapted the design of a dead-end pillar device by dividing the pillars into four zones, with the pillar gaps decreasing in each successive zone. This design allowed the cells to deform and regain their shapes as the cells moved from zone to zone. They isolated fetal nucleated red blood cells (fNRBC), which are less dense and stiffer than normal red blood cells, from maternal blood. The fNRBCs contained in the mononuclear cell layer, obtained after a prior centrifugation step, was used as the sample for this experiment. There is a recent report (Masuda et al. 2017) on a pillar-based open channel sorting device for isolation of CTCs from blood. In this design, the pillars were arranged in a hexagonal pattern, and the distance between pillars was chosen such that the target cell could easily be trapped in the hexagonal area between pillars. A major problem with CTC separation is the loss of these rare cells in the tubing connected to the microfluidic device. The open channel design developed by this group allowed direct recovery of the captured CTCs from the microfluidic chip by micropipette aspiration.

Other approaches to solve the problem of clogging in filter-based devices include integration of micropumps (Cheng et al. 2016), performing pneumatic actuation (Huang et al. 2014), or introducing mechanical vibrations using piezoelectric transducers (Yoon et al. 2016). These approaches, while effective in dislodging trapped cells, require either complex microfabrication steps or the integration of power sources and transducers into the device.

Deterministic Lateral Displacement

Deterministic lateral displacement (DLD) devices were developed (Huang et al. 2004) to overcome the low throughput and high clogging issues of size-exclusion separation devices. DLD is a pillar-based cell separation technique that separates cells based on size, as shown in Fig. 7. Unlike the other pillar-based devices, here the pillars in each row are displaced horizontally with respect to the previous row. Typically, the horizontal displacement ($\Delta\lambda$) is by a pre-determined fraction of the center-to-center distance (λ) of the pillars, which leads to a periodic arrangement. For example, if the lateral displacement ($\Delta\lambda$) between successive rows is $\lambda/3$, then the 1st and the 4th rows of pillars would be exactly aligned. In this device, particles with diameters smaller and larger than a critical diameter (D_c) follow different paths through the pillar network. Smaller particles continue along the same streamline, while larger particles are bumped from pillar to pillar, resulting in a lateral displacement (Inglis et al. 2006). The critical size (D_c) is related to the side-to-side gap between the pillars and the shift fraction ($\Delta\lambda/\lambda$). The DLD design allows fabrication of pillars with large gaps to sort cells with small size differences because the sorting ability of this device is directly proportional to shift fraction. Some variations in the pillar shapes have been reported in the literature. There is a report (Zeming et al.

Fig. 7 Schematic of the deterministic lateral displacement (DLD) device. The consecutive rows of pillars are laterally displaced with respect to the previous row by a pre-determined distance
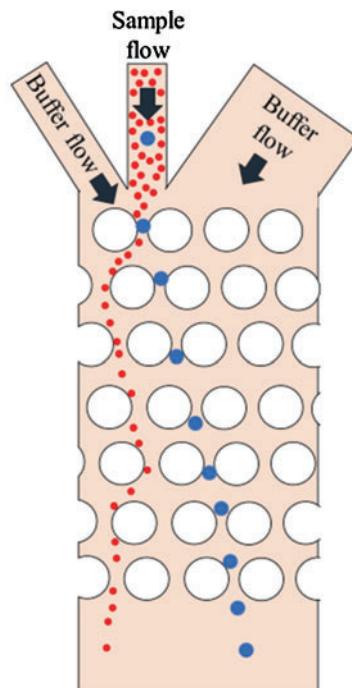
2013) on I-shaped pillars for sorting of non-spherical cells in the DLD design. The "I" shape of the pillars continuously rotated the cells, leading to the highest lateral migration of the biconcave RBCs.

DLD devices have been extensively used for the separation of rare cells. Huang and others (Huang et al. 2008) isolated nucleated RBCs from peripheral blood with a high throughput. Liu et al. (2013) used a DLD design for cancer cell enrichment prior to affinity-based separation. Another group (Au et al. 2017) used an asymmetric DLD approach to isolate CTC clusters from the blood. Their microfluidic chip consisted of two stages. The first stage had cylindrical micro-posts to deflect large particles. The second stage had one half of the pillars shaped as ellipsoids, and the half as I-shaped pillars to induce rotation of the CTC clusters for improved separation.
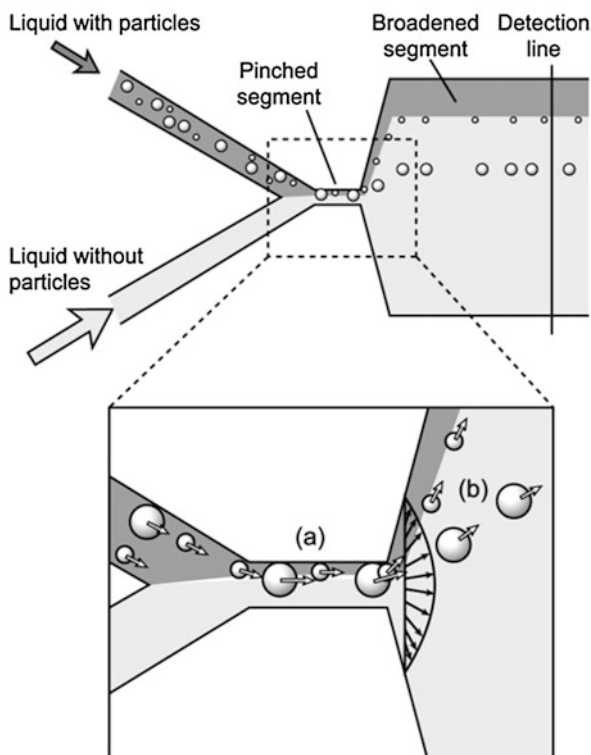
Hydrodynamic Separation

Hydrodynamic separation techniques rely on the fluid flow alone to sort particles based on size, shape, or deformability. Usually there are no obstacles placed in the flow path. In this chapter, we have divided the hydrodynamic separation techniques into two regimes: (a) when $Re \cong 0$ (*non-inertial regime*) and (b) when $1 < Re < 100$ (*inertial regime*).

Non-inertial Hydrodynamic Separation

These techniques rely on simple flow division in microfluidic channels at very low Reynolds numbers. Due to linearity of the system, particles do not move from one streamline to another in these devices. The *pinched flow fractionation* (PFF) is one such technique demonstrated by Yamada and others (Yamada et al. 2004). As shown in Fig. 8, there are two inlets in the device, one containing the mixture of the particles to be separated and the other containing a buffer without particles. Both the sample and the buffer flow into a narrow channel (i.e., the pinched region), which after a distance suddenly widens. The flow containing the particles is tightly focused by the buffer flow such that all particles line up against one sidewall of the pinched region. This is the most critical step in the PFF technique. At this point, the centers of the aligned small and the large particles lie on different streamlines.

When the particles enter the wider channel, they continue to move along their respective streamlines in the spreading flow profile. The small particles move along the wall, and the large particles move away from the wall, toward the center of the device. These particles can be detected according to their sizes in a direction perpendicular to the direction of the flow. A number of outlet channels placed at the end of the wide channel can then collect each cell fraction. In this technique, the separation efficiency is strongly dependent on the tightness of focusing of the sample flow in the pinched region. Another group (Pødenphant et al. 2015) used pinched

Fig. 8 Pinched flow fractionation. A buffer stream focuses the particle stream against the wall in the pinched channel. Due to the difference in their sizes, larger and smaller particles follow different streamlines when they are focused. When channel widens, smaller cells continue to flow near to the wall and larger cells shift near the center. As the cells of different sizes follow different streamlines in the laminar flow, they can be collected in different outlets. (Reproduced by permission of the ACS publications Yamada et al. 2004)
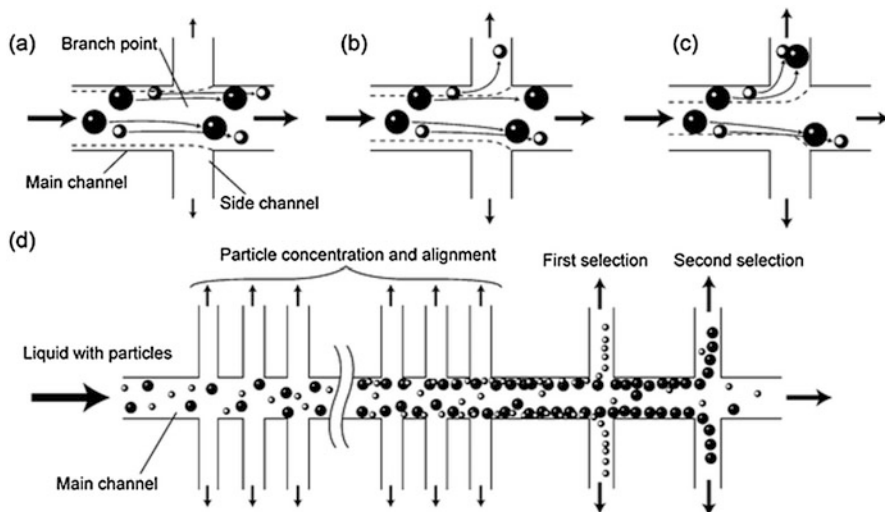
Fig. 9 Schematic diagram of hydrodynamic cell separation device. (Reproduced by permission of the Royal Society of Chemistry Yamada and Seki 2005)

flow fractionation to separate LS174T colon cancer cells from WBCs with a separation efficiency of 90%. A design improvement on symmetric PFF was proposed by Takagi and others (Takagi et al. 2005) by making the flow resistances of the outlet channels asymmetric (e.g., asymmetric pinched flow fractionation). This modification was carried out to allow particles with much smaller size differences (~1 μm) to be separated. They also observed that the shape of non-spherical cells plays a strong role in this separation technique. The smallest dimension of a non-spherical cell (e.g., the ~2 μm width of a discoid red blood cell) determines the extent of pinching required to separate it using this method. A problem with this method is that cells may be damaged during extreme squeezing against the sidewall. Another group (Lin et al. 2013) used a pinch-flow design to concentrate large target cells prior to sorting with ratchet-shaped pillar gaps. The separation was based on the difference in both size and deformability of the cells. They sorted UC13 bladder cancer cells from leukocytes with 97% yield and 3000-fold enrichment.

While PFF relied on flow focusing to line up the particles along one sidewall of a pinched channel, another technique from the same group (Yamada and Seki 2005) used the division of flow between the main channel and a number of perpendicular side channels to concentrate the particles near the sidewall (Fig. 9). This separation technique utilized the fact that the center of a particle cannot be positioned at any distance from the sidewall which is smaller than the radius of the particle. The division of flow among the main channel and the various side channels can be estimated using hydraulic circuit equations. If the "virtual width" of the flow segment entering the side channel is less than the particle diameter, the particle does not enter the side channel, even if the "physical width" of the side channel is greater than the particle diameter. The dimensions of the side channels and the flow rates were optimized to obtain the following three flow states with different virtual

widths of the side flow: (i) the side channel only draws in the liquid and concentrates the particles in the main channel, (ii) the side channel draws in the small particles, and (iii) the side channel draws in the large particles. Later this design was used to demonstrate the enrichment of leukocytes from 10X diluted blood. Recently an improvement (Yamada et al. 2017) on this design was proposed. The main and the side channels were integrated into an asymmetric lattice pattern that acted like a size-based sieve. The main channel is slanted at an angle with respect to the macroscopic flow, which further enhances the difference in the lateral positions of the small and the large cells. The slant angle of the side channel and the density of the liquid are the key design parameters in this device.

There is another class of hydrodynamic separation techniques at low Reynolds numbers where the particles in laminar flow can be made to move in directions transverse to the axial flow by introducing some nonlinear effect, such as elastic deformation of soft objects in a flow. Geislinger and others (Geislinger and Franke 2013) used a purely viscous non-inertial hydrodynamic effect to sort deformable blood cells. Their device consisted of a main channel and a side channel. The separation performance depended strongly on the size difference and somewhat less strongly on the difference in the shape and the deformability of the cells. The operation of this device was later demonstrated (Geislinger and Franke 2013) for sorting of melanoma cells from RBCs with an efficiency of 100%.

Inertial Hydrodynamic Separation

Inertial effects (Di Carlo et al. 2007; Nivedita and Papautsky 2013) become significant in microfluidic channels when the Reynolds number lies between 1 and 100. Under this condition, both viscosity and inertia terms must be taken into account when solving the Navier-Stokes equation to obtain the flow profile. The introduction of the inertial term allows cross-stream lateral migration of particles, which was not possible under purely Stoke's flow ($Re \cong 0$).

For the case of neutrally buoyant particles (e.g., cells in buffer or media) in a straight microfluidic channel, there are two kinds of inertial forces on the particles: (a) a wall lift force resulting from the interaction between the particle and walls that pushes the particles away from the wall and (b) a shear gradient lift force, resulting from the parabolic flow profile, that pushes the particles away from the center. Particles of different sizes experience different wall and shear gradient forces and, therefore, migrate away from the axis to different equilibrium positions in the lateral direction. These equilibrium positions are strongly dependent on the channel geometry. These inertial forces in straight channels lead to strong particle focusing. Hur and others (Hur et al. 2011) combined inertial focusing with microscale laminar vortices to separate spiked cancer cells from blood with a very high throughput. Another group (Parichehreh et al. 2013) combined aqueous phase partitioning and inertial focusing in a straight microchannel to enrich the population of nucleated cells in the blood. The flow of the blood sample in the microfluidic chip was flanked by the flow of a dextran phase on both sides. The RBCs preferentially migrated to the dextran layer toward the wall of the channels, while the WBCs remained near the center. This difference in the positions of RBCs and WBCs was later amplified by inertial microfluidics to achieve improved separation.

In addition to the lift forces, there is another force on particles in curved microchannels. Due to the parabolic flow profile, the fluid at the center of the channel is pushed outward due to the centrifugal force. To fulfill the incompressibility condition, the fluid from the sides of the channel moves toward the center. This sets up two symmetric vortices in the top and the bottom halves of the channel, leading to a secondary flow called the Dean flow. Larger channel widths, higher curvature, and higher flow velocities lead to higher Dean flows. Microchannels with spiral and serpentine geometries have been designed to separate cells based on the equilibrium between the inertial lift and the Dean forces. The ratio (R_f) between the inertial lift and the Dean forces varies as the square of the particle diameter. Therefore, particles of different sizes move to different radial equilibrium positions, leading to a size-based separation.

Several variations of the basic spiral cell separation device have been reported in the literature. A double spiral geometry (Sun et al. 2012) was developed to improve the separation resolution. Its performance was demonstrated by separating spiked tumor cells from diluted blood. Zhou and others (Zhou et al. 2013) modulated the channel aspect ratio. An initial high aspect ratio segment was used first to focus the particles. Then a later low aspect ratio segment separated the particles according to their sizes. They spiked and isolated prostate epithelial tumor cells from the blood. A spiral device with a trapezoidal cross-section (Warkiani et al. 2014) was designed to improve the sorting performance. The height of the outer channel wall was greater than that of the inner wall, leading to a trapezoidal cross-section. The inlet to the channel was placed at the outside of the spiral. The blood with lysed RBCs and spiked with circulating tumor cells (CTCs) was introduced at the inlet and separated with an ultrahigh throughput (7.5 ml of the blood in 8 min). The large CTCs were focused near the inner wall of the spiral channel, and the smaller WBCs were focused near the outer wall. One major limitation of the inertial focusing technique for clinical applications is the need to heavily dilute blood to reduce cell-cell interactions.

Microfluidic Active Separation Techniques

Unlike passive techniques, where the cell separation is carried out using microscale obstacles or the fluid flow alone, active separation techniques require the use of an external field (e.g., electric, optical, magnetic, acoustic, etc.). We discuss a few of the most common active separation techniques here.

Dielectrophoresis (DEP)

Dielectrophoresis is a separation technique based on the intrinsic polarizability of the cells. Polarizable particles, when placed in a nonuniform electric field, move either toward higher or lower field regions depending on the sign of their Clausius-Mossotti (CM) factor. If polarizability of the particle is higher than the polarizability of the buffer medium in which it is suspended, the particle moves toward the higher electric field. This phenomenon is known as positive dielectrophoresis (pDEP). On the other hand, if the polarizability of the particle is lower than that of the medium,
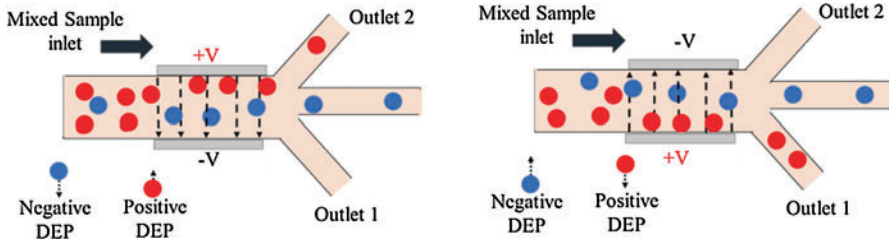
Fig. 10 Schematic diagram explaining dielectrophoresis (DEP). In positive DEP, particles move toward the higher electric field. In negative DEP, the particles move toward the electric field minima

the particle moves toward the weaker electric field. This phenomenon is called negative dielectrophoresis (nDEP) (Gossett et al. 2010). The DEP force depends strongly on the size of the cell and can be used for size-based sorting. The equilibrium position of a particle in the flow depends on the relative magnitudes of the DEP and the drag forces. The cells expressing negative DEP are carried away by the flow, while the cells expressing positive DEP are retained in the channel by the electric field gradient.

When an AC electric field is used for DEP (Fig. 10) instead of a DC field, the electrochemical reactions at the electrodes are minimized. In addition, cells can be sorted based on both their size and frequency response. Particles have a positive CM factor in some frequency ranges and a negative CM factor in other frequencies. The frequency at which the CM factor changes its sign is called the crossover frequency. Mammalian cells show negative DEP at low frequencies in the 10 kHz to 1 MHz frequency range and positive DEP at the higher frequencies. A mixture of particles can be separated based on their crossover frequency. Vykoukal and others (Vykoukal et al. 2009) measured the specific membrane capacitances of leukocyte subpopulations using crossover frequency measurements.

Recently a high-throughput DEP was demonstrated (Faraghat et al. 2017) to separate spiked cancer cells from RBCs. Another report (Antfolk et al. 2017) used DEP to trap and sort spiked prostate cancer cells (DU145) in blood. The sample was pre-concentrated by acoustophoresis prior to sorting. Elvington and others (Elvington et al. 2013) reported a contactless DEP technique to eliminate problems, such as bubble formation and electrolysis. In contactless DEP, there is no direct contact between metallic electrodes and the sample. Instead of a metallic electrode, a fluid electrode is capacitively coupled to an AC voltage source. The highest throughput obtained with DEP is still lower than other cell separating techniques, such as inertial sorting. Another disadvantage is that DEP requires the fabrication of integrated planar electrodes in the microfluidic channel. Wang and others (Wang et al. 2000) developed a DEP-FFF system for the separation of breast cancer cells from $CD34^+$ hematopoietic stem cells and from T lymphocytes. Their device consisted of a chamber equipped with an array of microfabricated interdigitated electrodes at the bottom. Hu and others (Hu et al. 2005) demonstrated >200-fold enrichment of rare cells by DEP in a microfluidic device.

Magnetic Separation

The idea of magnetic separation in a microfluidic channel originated from MACS. Magnetic separation of blood cells looked promising due to the inherent magnetic properties of the WBCs and the RBCs. WBCs are diamagnetic, and RBCs may be diamagnetic (oxyhemoglobin state) or paramagnetic (deoxyhemoglobin state). Furlani (2007) fabricated a microfluidic channel by embedding an array of permalloy elements underneath it, which could be magnetized using an external bias field. It led to a nonuniform field distribution. Separation of WBCs and deoxygenated RBCs was demonstrated in this device. Cells that are not intrinsically magnetic can be labeled with magnetic nanoparticles. Pamme and Wilhelm (2006) magnetically labeled mouse macrophages and HeLa cells following the endocytic pathway of the cells. A magnetic field was applied perpendicular to the flow direction in a microfluidic chip. The magnetically labeled cells were deflected toward the magnet, while the non-labeled cells flowed toward the outlet.

Acoustophoresis

Acoustophoresis uses ultrasound waves to separate cells. If standing waves of ultrasound are produced in a microchannel, then cells either move to a pressure node or an antinode depending on the property of the cells. The acoustic force on a cell depends on its volume, relative density between the cell and the surrounding fluid, and their relative compressibility. It also depends on the radiation pressure, the wavelength of the sound, and a contrast factor. Most mammalian cells move to the nodes under the action of this force. If the half wavelength of a standing wave matches the channel width, a pressure node is formed at the center, and antinodes are created near the walls. As a result, cells with negative contrast move to the center and are carried away by the laminar flow through a central outlet. The cell-free liquid can be collected through peripheral outlets. A similar concept has been used to separate plasma from blood (Lenshof et al. 2009).

Figure 11 shows how acoustophoresis may be used for single-cell separation. The acoustic radiation force acting on particles of different sizes, but same densities, will focus the particles in the same region of the channel. As the force varies with the volume of the cell, cells of different sizes will cross the streamlines at different rates. There is a recent report (Shields IV et al. 2014) on using acoustophoresis for capture

Fig. 11 Single rare cell separation using surface acoustic waves from the mixed cell population
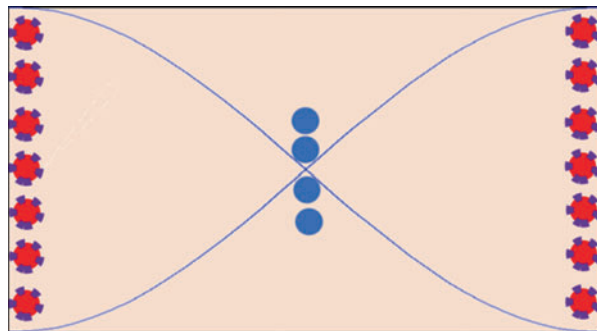
of cells using elastomeric particles. Elastomeric particles tend to move to the channel walls (antinodes). If cells can be bound to elastomeric particles by immunological labeling in such a way that the force on the particles is greater than the force on the cells, then the particles carry these cells to the antinodes, e.g., the channel walls, of acoustic standing waves. Unlabelled cells at the pressure nodes can be carried away by the flow. Another group (Augustsson et al. 2012) used microfluidic acoustophoresis to separate prostate cancer cells from blood using an additional acoustic pre-alignment procedure.

Affinity-Based Separation

Affinity-based cell separation uses labels, typically based on antigen-antibody interactions. The microfluidic chip is modified with a specific antibody which is capable of binding to the antigen on the surface of the desired cell. When the sample passes through the microfluidic chip, the desired cell is captured, while the rest of the sample is collected at the outlet. Finally, the immobilized cell is eluted from the microchannels for analysis. This technique has much better sensitivity and specificity compared to the other label-free techniques due to the use of labels specific to the target cell (Hu et al. 2016). An affinity-based microfluidic chip was successfully demonstrated by the Toner group (Nagrath et al. 2007) for the separation of epithelial CTCs from whole blood. The CTC-chip consisted of 78,000 micro-posts which were coated with the anti-epithelial cell adhesion molecule (EpCAM). The large number of micro-posts increased the surface area for binding compared to a straight microfluidic channel. The chip was clinically tested on patients with metastatic prostate, lung, breast, and colon cancer. It detected CTCs in 115 of 116 (99%) samples. Later, same group developed a herringbone-chip (HB-chip) with high throughput (Stott et al. 2010). The design was chosen such that it introduces chaotic flow in the device which further increases the cell-to-surface interaction. Another group (Sarkar et al. 2016) reported a continuous flow and high-throughput microfluidic device based on combining inertial microfluidics and affinity separation. Liu and others (Liu et al. 2013) demonstrated an integrated microfluidic chip for CTC separation from blood separation combining deterministic lateral displacement and affinity-based techniques. Breast cancer cells were spiked in the blood sample and separated with an enrichment factor of 1500X, a throughput of 9.6 ml/min, capture yield of 90%, and purity of 50%. Murlidhar et al. (2014) reported an affinity-based ultrahigh-throughput CTC capture device (Onco-Bean chip). Bean-shaped pillars were designed to increase the interaction between the antibody-coated pillars and circulating tumor cells. The pillars were arranged radially, reducing the shear along the axis of cell movement and thus allowing increased affinity-based capture of CTCs. Each successive row along the radius was displaced randomly to improve the interaction between CTCs and micro-posts. This device achieved an ultrahigh throughput of 10 ml/hr. Cells were sorted with an efficiency greater than 80%. The recovered cells were tested for viability, and 93% of the cells were found to be viable. Sheng and others (Sheng et al. 2012) used aptamers in combination with a

Table 2 Parameters to quantify the efficiency of conventional cell separation techniques

Method	Flow rate (ml/min)	Purity (%)	Recovery (%)	Enrichment (fold)	Throughput (cells/s)	References
Centrifugation	–	95–97	40–90	–	–	Boyum 1977
Fluorescence-activated cell sorting (FACS)	–	90	–	–	10,000	(Bonner et al. 1972; Lee et al. 2017)
Magnetic-activated cell sorting (MACS)	8	–	>90	>100	–	Miltenyi et al. 1990

pillar-based microfluidic chip for tumor cell separation from whole blood with a capture efficiency of >95% and purity of ~ 81%. The device consisted of >59,000 micropillars to improve the cell-to-surface interaction. The same group (Sheng et al. 2014) later implemented geometrically enhanced mixing in the micro-fluidic chip prior to cancer cell separation to improve the purity and the capture efficiency. This device achieved a tumor cell capture efficiency of >90% and purity of >84% by increasing the groove widths.

Comparison Between Different Microfluidic Separation Techniques

As shown in Table 2, non-inertial hydrodynamic separation, deterministic lateral displacement, and dielectrophoresis techniques have reported the highest capture efficiencies, nearing 100% (Geislinger and Franke 2013; Antfolk et al. 2017; Huang et al. 2008). On the other hand, deterministic lateral displacement, non-inertial hydrodynamic, and acoustophoresis techniques achieved the highest cell recovery (nearly ~99%) (Au et al. 2017; Lin et al. 2013; Pødenphant et al. 2015; Augustsson et al. 2012). However, inertial hydrodynamic, membrane, and pillar-based separa-tion techniques also reported recoveries in excess of ~90% (Parichehreh et al. 2013; Tang et al. 2014; Masuda et al. 2017). The recovery in dielectrophoresis was somewhat lower (~76%), which can be improved by optimizing the flow rates (Antfolk et al. 2017). The highest purity for the separated cells was reported to be ~99%, achieved by dielectrophoresis and acoustophoresis (Antfolk et al. 2017; Augustsson et al. 2012). The enrichment factor of 3000-fold and throughput 9.6 ml/min have been achieved highest by hydrodynamic and affinity based (Lin et al. 2013; Liu et al. 2013). In comparison, each individual technique appears to excel in at most one or two separation parameters. We believe that by combining two or more techniques in an experiment, all the separation parameters can be improved (Table 3).

Table 3 Comparison of microfluidic techniques

Techniques	Separation criteria	Flow rate (mL/min)	Capture/Separation efficiency (%)	Recovery (%)	Purity (%)	Enrichment (fold)	Throughput (mL/min)	References
Dielectrophoresis	Size, density, polarizability	4×10^{-3}	100	~76	100	–	0.08	Antfolk et al. 2017
		5×10^{-3}	–	–		–	–	Elvington et al. 2013
		0.3	–	–		>200	–	Hu et al. 2005
		0.5	–	70	92	35	–	Wang et al. 2000
Affinity-based separation	Size, affinity	0.016	65	–	50	10^6	0.03	Nagrath et al. 2007
		1.6	90	–	50	1500	9.6	Liu et al. 2013
		0.016	>80	–	–	–	0.16	Murlidhar et al. 2014
		3.6×10^{-3}	95		~81	–	0.035	Sheng et al. 2012
		0.06	>90	–	84	–	0.6	Sheng et al. 2014
Pillar-based separation	Size, deformability	5.8×10^{-3}	–	–	–	–	–	Mohamed et al. 2007
		0.16–0.33	–	90.6	60	–	0.04–0.08	Masuda et al. 2017
		6×10^{-6}	98 (MLC), 97 (PBMC)		99 (MLC) 95 (PBMC)	–	–	McFaul et al. 2012
		6.5×10^{-4}	–	–	–	–	–	VanDelinder and Groisman 2006

Table 3 (continued)

Techniques	Separation criteria	Flow rate (mL/min)	Capture/Separation efficiency (%)	Recovery (%)	Purity (%)	Enrichment (fold)	Throughput (mL/min)	References
Inertial hydrodynamic separation	Size	0.03	–	90	–	–	–	Parichehreh et al. 2013
		–	96.8	88.5	–	15	0.33	Sun et al. 2012
		0.1	>99	–	>90	–	–	Zhou et al. 2013
Non-inertial hydrodynamic separation	Size	5×10^{-4} – 8.3×10^{-4}	90	–	–	–	–	Podenphant et al. 2015
		0.01	100	–	–	46	–	Geislinger and Franke 2013
		–	97	–	–	3000	8.33×10^{-6}	Lin et al. 2013
Membrane-based separation	Size, deformability	0.2–2	>95	–	–	–	–	Tang et al. 2014
		–	100	98	–	–	–	Yoon et al. 2016
Deterministic lateral displacement	Size	2×10^{-4}	100	–	–	–	–	Zeming et al. 2013
		8.3×10^{-3}	–	99	–	–	0.05–0.02	Au et al. 2017
		0.45	100	>95	–	10–20	0.42–0.05	Huang et al. 2008
Acoustophoresis	Size, density	0.56	–	93.6–97.9 (for fixed cells) 72.5–93.9 (for nonfixed)	97.4–98.4 (for fixed cells) 79.6–99.7 (for nonfixed)	–	–	Augustsson et al. 2012

Conclusion

Single-cell separation techniques play a major role in the diagnosis of diseases. In the chapter, we have discussed the state-of-the-art conventional and microfluidic cell separation techniques. Microfluidic techniques that are based on physical properties (e.g., deformability, size, polarizability, magnetic susceptibility, etc.) do not require any labeling. Compared to label-free techniques, affinity-based rare cell separation shows better separation performance. The interaction between the antibody-coated microfluidic channel and the antigens on the target cell surface was further strengthened by the introduction of pillars to increase the surface-to-volume ratio. Another challenge in single-cell separation is the preprocessing of clinical samples. Most of the techniques discussed here needed a dilution of blood samples, which added an extra processing step. More single-cell separation techniques that work with sample without preprocessing (e.g., whole blood) need to be developed. The microfluidic separation techniques that we reviewed are still at the laboratory level or the proof-of-concept stage. Though some of the microfluidic devices have reached clinical trials, these devices are still not widely used in the settings for which these were originally developed. There is still a strong need for microfluidic single-cell separation techniques which are affordable, reliable in clinical settings, and capable of replacing the existing techniques.

References

Antfolk M, Kim SH, Koizumi S et al (2017) Label-free single-cell separation and imaging of cancer cells using an integrated microfluidic system. Sci Rep 7:1–12. https://doi.org/10.1038/srep46507

Au SH, Edd J, Stoddard AE et al (2017) Microfluidic isolation of circulating tumor cell clusters by size and asymmetry. Sci Rep 7:1–10. https://doi.org/10.1038/s41598-017-01150-3

Augustsson P, Magnusson C, Nordin M et al (2012) Microfluidic, label-free enrichment of prostate cancer cells in blood based on acoustophoresis. Anal Chem 84:7954–7962. https://doi.org/10.1021/ac301723s

Beebe DJ, Mensing GA, Walker GM (2002) Physics and applications of microfluidics in biology. Annu Rev Biomed Eng 4:261–286. https://doi.org/10.1146/annurev.bioeng.4.112601.125916

Bonner WA, Hulett HR, Sweet RG, Herzenberg LA (1972) Fluorescence activated cell sorting. Rev Sci Instrum 43(3):404–409. https://doi.org/10.1063/1.1685647

Boyum A (1977) Separation of lymphocytes, lymphocyte subgroups and monocytes: a review. Lymphology 10(2):71–76

Brody JP, Osborn TD, Forster FK et al (1996) A planar microfabricated fluid filter. Sensors Actuators A Phys 54(1–3):704–708. https://doi.org/10.1016/S0924-4247(97)80042-8

Chen X, Cui DF, Liu CC, Li H (2008) Microfluidic chip for blood cell separation and collection based on crossflow filtration. Sensors Actuators B Chem 130:216–221. https://doi.org/10.1016/j.snb.2007.07.126

Cheng Y, Ye X, Ma Z, Xie S, Wang W (2016) High-throughput and clogging-free microfluidic filtration platform for on-chip cell separation from undiluted whole blood. Biomicrofluidics 10(1):014118. https://doi.org/10.1063/1.4941985

Crowley TA, Pizziconi V (2005) Isolation of plasma from whole blood using planar microfilters for lab-on-a-chip applications. Lab Chip 5:922. https://doi.org/10.1039/b502930a

Datta S, Malhotra L, Dickerson R et al (2015) Laser capture microdissection: big data from small samples. Histol Histopathol 30:1255–1269. https://doi.org/10.14670/HH-11-622.Laser

Di Carlo D, Irimia D, Tompkins RG, Toner M (2007) Continuous inertial focusing, ordering, and separation of particles in microchannels. Proc Natl Acad Sci 104:18892–18897. https://doi.org/10.1073/pnas.0704958104

Elvington ES, Salmanzadeh A, Stremler MA, Davalos RV (2013) Label-free isolation and enrichment of cells through contactless dielectrophoresis. J Vis Exp:1–10. https://doi.org/10.3791/50634

Emmert Buck MR, Bonner RF, Smith PD et al (1996) Laser capture microdissection. Science 274(5289):998–1001. https://doi.org/10.1126/science.274.5289.998

Faraghat SA, Hoettges KF, Steinbach MK et al (2017) High-throughput, low-loss, low-cost, and label-free cell separation using electrophysiology-activated cell enrichment. Proc Natl Acad Sci 114:4591–4596. https://doi.org/10.1073/pnas.1700773114

Fend F, Raffeld M (2000) Laser capture microdissection in pathology. J Clin Pathol 53:666–672. https://doi.org/10.1136/jcp.53.9.666

Furlani EP (2007) Magnetophoretic separation of blood cells at the microscale. J Phys D 40(5):1313. https://doi.org/10.1088/0022-3727/40/5/001

Geislinger TM, Franke T (2013) Sorting of circulating tumor cells (MV3-melanoma) and red blood cells using non-inertial lift. Biomicrofluidics 7:1–9. https://doi.org/10.1063/1.4818907

Gossett DR, Weaver WM, MacH AJ et al (2010) Label-free cell separation and sorting in microfluidic systems. Anal Bioanal Chem 397:3249–3267. https://doi.org/10.1007/s00216-010-3721-9

Herzenberg LA, Sweet RG (1976) Fluorescence activated cell sorting. Rev Sci Instrum 234:108–117. https://doi.org/10.1063/1.1685647

Herzenberg LA, Parks D, Sahaf B et al (2002) The history and future of the fluorescence activated cell sorter and flow cytometry: a view from Stanford. Clin Chem 48:1819–1827. https://doi.org/10.1038/scientificamerican0376-108

Hu X, Bessette PH et al (2005) Marker-specific sorting of rare cells using dielectrophoresis. Proc Natl Acad Sci U S A 102(44):15757–15761. https://doi.org/10.1073/pnas.0507719102

Hu P, Zhang W, Xin H, Deng G (2016) Single cell isolation and analysis. Front Cell Dev Biol 4:1–12. https://doi.org/10.3389/fcell.2016.00116

Huang LR, Cox EC, Austin RH, Sturm JC (2004) Continuous particle separation through deterministic lateral displacement. Science 304(5673):987–991. https://doi.org/10.1126/science.1094567

Huang R, Barber TA, Schmidt MA et al (2008) A microfluidics approach for the isolation of nucleated red blood cells (NRBCs) from the peripheral blood of pregnant women. Prenat Diagn 28(10):892–899. https://doi.org/10.1002/pd.2079

Huang SB, Zhao Y, Chen D et al (2014) A clogging-free microfluidic platform with an incorporated pneumatically driven membrane-based active valve enabling specific membrane capacitance and cytoplasm conductivity characterization of single cells. Sensors Actuators B Chem 190:928–936. https://doi.org/10.1016/j.snb.2013.09.070

Hulett HR, Bonner WA, Barrett J et al (1969) Cell sorting: automated separation of mammalian cells as a function of intracellular fluorescence. Science 166(3906):747–749. https://doi.org/10.1126/science.166.3906.747

Hur SC, Mach AJ, Di Carlo D (2011) High-throughput size-based rare cell enrichment using microscale vortices. Biomicrofluidics 5:1–10. https://doi.org/10.1063/1.3576780

Inglis DW, Davis JA, Austin RH, Sturm JC (2006) Critical particle size for fractionation by deterministic lateral displacement. Lab Chip 6:655. https://doi.org/10.1039/b515371a

Ji HM, Samper V, Chen Y et al (2008) Silicon-based microfilters for whole blood cell separation. Biomed Microdevices 10:251–257. https://doi.org/10.1007/s10544-007-9131-x

Lee W, Tseng P, Di Carlo D (2017) Microfluidic cell sorting and separation technology. In: Lee W, Tseng P, Di Carlo D (eds) Microtechnology for cell manipulation and sorting. Microsystems and nanosystems. Springer, Cham

Lenshof A, Ahmad-Tajudin A, Järås K, Swärd-Nilsson AM et al (2009) Acoustic whole blood plasmapheresis chip for prostate specific antigen microarray diagnostics. Anal Chem 81(15):6030–6037. https://doi.org/10.1021/ac9013572

Lin BK, McFaul SM, Jin C et al (2013) Highly selective biomechanical separation of cancer cells from leukocytes using microfluidic ratchets and hydrodynamic concentrator. Biomicrofluidics 7:17–20. https://doi.org/10.1063/1.4812688

Liu Z, Zhang W, Huang F et al (2013) High throughput capture of circulating tumor cells using an integrated microfluidic system. Biosens Bioelectron 47:113–119. https://doi.org/10.1016/j.bios.2013.03.017

Masuda T, Song W, Nakanishi H et al (2017) Rare cell isolation and recovery on open- channel microfluidic chip. PLoS One 12:1–14. https://doi.org/10.1371/journal.pone.0174937

McFaul SM, Lin BK, Ma H (2012) Cell separation based on size and deformability using microfluidic funnel ratchets. Lab Chip 12:2369. https://doi.org/10.1039/c2lc21045b

Mehendale N, Sharma O, D'Costa C, Paul D (2018) A radial pillar device (RAPID) for continuous and high-throughput separation of multi-sized particles. Biomed Microdevices 20:1–9. https://doi.org/10.1007/s10544-017-0246-4

Miltenyi S, Müller W, Weichel W, Radbruch A (1990) High gradient magnetic cell separation with MACS. Cytometry 11:231–238. https://doi.org/10.1002/cyto.990110203

Mohamed H, Turner JN, Caggana M (2007) Biochip for separating fetal cells from maternal circulation. J Chromatogr A 1162:187–192. https://doi.org/10.1016/j.chroma.2007.06.025

Murlidhar V, Zeinali M, Grabauskiene S et al (2014) A radial flow microfluidic device for ultra-high-throughput affinity-based isolation of circulating tumor cells. Small 10:4895–4904. https://doi.org/10.1002/smll.201400719

Nagrath S, Sequist LV, Maheswaran S et al (2007) Isolation of rare circulating tumour cells in cancer patients by microchip technology. Nature 450:1235–1239. https://doi.org/10.1038/nature06385.Isolation

Nivedita N, Papautsky I (2013) Continuous separation of blood cells in spiral microfluidic devices. Biomicrofluidics 7(5):054101. https://doi.org/10.1063/1.4819275

Pamme N, Wilhelm C (2006) Continuous sorting of magnetic cells via on-chip free-flow magnetophoresis. Lab Chip 6(8):974–980. https://doi.org/10.1039/B604542A

Parichehreh V, Medepallai K, Babbarwal K, Sethu P (2013) Microfluidic inertia enhanced phase partitioning for enriching nucleated cell populations in blood. Lab Chip 13:892. https://doi.org/10.1039/c2lc40663b

Pødenphant M, Ashley N, Koprowska K et al (2015) Separation of cancer cells from white blood cells by pinched flow fractionation. Lab Chip 15:4598–4606. https://doi.org/10.1039/C5LC01014D

Sarkar A, Hou HW, Mahan AE et al (2016) Multiplexed affinity-based separation of proteins and cells using inertial microfluidics. Sci Rep 6:1–9. https://doi.org/10.1038/srep23589

Sheng W, Chen T, Kamath R, Xiong X et al (2012) Aptamer-enabled efficient isolation of cancer cells from whole blood using a microfluidic device. Anal Chem 84(9):4199–4206. https://doi.org/10.1021/ac3005633

Sheng W, Ogunwobi O, Chen T, Zhang J (2014) Capture, release and culture of circulating tumor cells from pancreatic cancer patients using an enhanced mixing chip. Lab Chip 14:89–98. https://doi.org/10.1039/c3lc51017d.Capture

Shields CW IV, Johnson LM, Gao L, López GP (2014) Elastomeric negative acoustic contrast particles for capture, acoustophoretic transport, and confinement of cells in microfluidic systems. Langmuir 30:3923–3927. https://doi.org/10.1021/la404677w

Songjaroen T, Dungchai W, Chailapakul O, Henry CS et al (2012) Blood separation on microfluidic paper-based analytical devices. Lab Chip 12(18):3392–3398. https://doi.org/10.1039/C2LC21299D

Stone HA, Kim S (2001) Microfluidics: basic issues, applications, and challenges. AICHE J 47(6):1250–1254. https://doi.org/10.1002/aic.690470602

Stott SL, Hsu C-H, Tsukrov DI et al (2010) Isolation of circulating tumor cells using a microvortex-generating herringbone-chip. Proc Natl Acad Sci 107(43):18392–18397. https://doi.org/10.1073/pnas.1012539107

Sun J, Li M, Liu C et al (2012) Double spiral microchannel for label-free tumor cell separation and enrichment. Lab Chip 12:3952. https://doi.org/10.1039/c2lc40679a

Takagi J, Yamada M, Yasuda M, Seki M (2005) Continuous particle separation in a microchannel having asymmetrically arranged multiple branches. Lab Chip 5:778. https://doi.org/10.1039/b501885d

Tang Y, Shi J, Li S et al (2014) Microfluidic device with integrated microfilter of conical-shaped holes for high efficiency and high purity capture of circulating tumor cells. Sci Rep 4:1–7. https://doi.org/10.1038/srep06052

VanDelinder V, Groisman A (2006) Separation of plasma from whole human blood in a continuous cross-flow in a molded microfluidic device. Anal Chem 78:3765–3771. https://doi.org/10.1021/ac060042r

VanDelinder V, Groisman A (2007) Perfusion in microfluidic cross-flow: separation of white blood cells from whole blood and exchange of medium in a continuous flow. Anal Chem 79:2023–2030. https://doi.org/10.1021/ac061659b

Vykoukal DM, Gascoyne PRC, Vykoukal J (2009) Dielectric characterization of complete mononuclear and polymorphonuclear blood cell subpopulations for label-free discrimination. Integr Biol 1:477. https://doi.org/10.1039/b906137a

Wachtel S, Shulman L, Sammons D (2001) Fetal cells in maternal blood. Clin Genet 59:74–79. https://doi.org/10.1034/j.1399-0004.2001.590202.x

Wang X-B et al (2000) Cell separation by dielectrophoretic field-flow-fractionation. Anal Chem 72(4):832–839. https://doi.org/10.1021/ac990922o

Warkiani ME, Guan G, Luan KB et al (2014) Slanted spiral microfluidics for the ultra-fast, label-free isolation of circulating tumor cells. Lab Chip 14:128–137. https://doi.org/10.1039/C3LC50617G

Wilding P, Kricka LJ, Cheng J, Hvichia G et al (1998) Integrated cell isolation and polymerase chain reaction analysis using silicon microfilter chambers. Anal Biochem 257(2):95–100. https://doi.org/10.1006/abio.1997.2530

Yamada M, Seki M (2005) Hydrodynamic filtration for on-chip particle concentration and classification utilizing microfluidics. Lab Chip 5:1233. https://doi.org/10.1039/b509386d

Yamada M, Nakashima M, Seki M (2004) Pinched flow fractionation: continuous size separation of particles utilizing a laminar flow profile in a pinched microchannel. Anal Chem 76:5465–5471. https://doi.org/10.1021/ac049863r

Yamada M, Seko W, Yanai T et al (2017) Slanted, asymmetric microfluidic lattices as size-selective sieves for continuous particle/cell sorting. Lab Chip 17:304–314. https://doi.org/10.1039/C6LC01237J

Yoon Y, Kim S, Lee J et al (2016) Clogging-free microfluidics for continuous size-based separation of microparticles. Sci Rep 6:1–8. https://doi.org/10.1038/srep26531

Zeming KK, Ranjan S, Zhang Y (2013) Rotational separation of non-spherical bioparticles using I-shaped pillar arrays in a microfluidic device. Nat Commun 4:1625–1628. https://doi.org/10.1038/ncomms2653

Zhou J, Giridhar PV, Kasper S, Papautsky I (2013) Modulation of aspect ratio for complete separation in an inertial microfluidic channel. Lab Chip 13:1919. https://doi.org/10.1039/c3lc50101a